Journal of Alloys and Compounds 652 (2015) 479–495

Contents lists available at ScienceDirect

Journal of Alloys and Compounds

journal homepage: http://www.elsevier.com/locate/jalcom

Magnetic order-disorder phase transition in $Cr_{70}Fe_{30}$ thin films

B. Ravi Kumar, S.N. Kaul*

School of Physics, University of Hyderabad, Central University P.O., Hyderabad 500046, Telangana, India

ARTICLE INFO

Article history:
Received 3 July 2015
Accepted 21 August 2015
Available online 22 August 2015

Keywords:
Critical phenomena
Critical exponents
Magnetic phase transition
Linear and non-linear ac magnetic susceptibilities
Cr–Fe alloys
Thin films

ABSTRACT

Dynamic magnetic response of $Cr_{70}Fe_{30}$ thin films with thickness in the range 11 nm $\leq t \leq$ 978 nm and composition above the critical concentration for ferromagnetism was determined by measuring linear (χ_1) and nonlinear ($\chi_2 - \chi_5$) ac-magnetic susceptibilities over three decades of frequency ($10^1 - 10^4$ Hz) in the temperature range 2–300 K. An elaborate analysis of $\chi_1(T)$, measured in the absence or presence of a superposed dc magnetic field, H_{dc}, reveals that the asymptotic critical behavior of the films with $t \geq 21$ nm is that of a three-dimensional (3D) isotropic dipolar ferromagnet. Interplay between long-range dipole–dipole and short-range exchange interactions causes a crossover to the 3D isotropic Heisenberg critical behavior when the temperature is increased above the Curie temperature, T_C, outside the asymptotic critical region (ACR). By contrast, in the ACR, the film with $t = 11$ nm behaves as a 3D Ising ferromagnet. T_C decreases with film thickness in accordance with the finite-size scaling with the value for the spin–spin correlation length exponent that corresponds to the 3D isotropic dipolar universality class. In the films with $t \leq 42$ nm, besides the macroscopic length scale of the ferromagnetic order in the static limit, there exists a length scale that corresponds to finite spin clusters, whose dynamics is spin glass-like.

1. Introduction

The alterations in the spin structure and the evolution of magnetic order with the addition of Fe to the spin density wave (SDW) antiferromagnet, Cr, in bulk $Cr_{100-x}Fe_x$ alloys, studied by experimental techniques such as Mössbauer effect, small-angle neutron scattering, inelastic/quasielastic neutron scattering, low-field magnetization and ac magnetic susceptibility, have been a subject of numerous publications [1–17] over the past four decades. Based on the results obtained till 1983, Burke and coworkers [5–7] have compiled the magnetic phase diagram for $Cr_{100-x}Fe_x$ alloys. According to this phase diagram, SDW antiferromagnetic order persists till 16.0(5) at. % Fe, spin glass-like behavior occurs in the range between 16 and 19 at. % Fe and ferromagnetism is prevalent above 19 at. % Fe. The part of the phase diagram that exclusively pertains to Fe concentrations $\gtrsim$20 at. % Fe, has been revisited several times subsequently to ascertain the nature of magnetic ground state and the transition from ferromagnetic (FM) to paramagnetic (PM) state. However, all such attempts have proved inconclusive. This is so because there is experimental evidence both in favor of [1–4,7,9,10,13] and against [11,12,14] the existence of long-range FM order and a well-defined FM-PM phase transition. The situation is further complicated by the observation that the $Cr_{100-x}Fe_x$ alloys have a strong tendency for segregation into Cr-rich and Fe-rich phases. Anomalously large values [2] for the critical exponents (that characterize the FM-PM phase transition) and a large but finite [3,4,7,9,10] spin–spin correlation length at the Curie temperature, T_C, have been attributed to the magnetic inhomogeneity that results from the phase segregation. Recognizing magnetic homogeneity as a prerequisite for unraveling the true intrinsic magnetic behavior, a systematic study of the effect of chemical short-range order (clustering) on magnetic properties within and outside the critical region has been initiated [15–17] a decade ago. Different post-synthesis annealing protocols and post-annealing quenching rates (to suppress phase segregation) [15–17] and optimum ion-beam sputtering conditions [18,19] have subsequently been employed for improving magnetic homogeneity in $Cr_{75-x}Fe_{25+x}$ ($x = 0, 5$) alloys in the bulk and thin film forms, respectively. The investigations of the critical behavior near the FM-PM phase transition in the alloys, so synthesized, have indicated that, in the bulk [15–17] and irrespective of the film thickness [18], these systems behave as a two-dimensional ($d = 2$) Ising ferromagnet in which attractive isotropic 'long-range' interactions between spins decay with distance (r) as $J(r) \sim r^{-(d+\sigma)}$ with $\sigma = 1.4$. This result is counter intuitive because a $d = 2$ critical behavior is

* Corresponding author.
E-mail address: kaulsp@uohyd.ac.in (S.N. Kaul).

http://dx.doi.org/10.1016/j.jallcom.2015.08.173
0925-8388/

claimed to occur in a $d = 3$ system (bulk). Furthermore, the values of the critical exponents determined for the bulk and thin films assert that these systems do not fall within any known universality class. Since most of the previous critical behavior determinations involved application of strong dc fields, it is not clear if the observed critical behavior is *intrinsic* or *field-induced*. The main aim of this work is to resolve the controversy surrounding the FM-PM phase transition and find out if the spatial dimensionality crossover effects play a role in governing the critical phenomena in the $Cr_{100-x}Fe_x$ thin films with $x \gtrsim 20$ at. % Fe. The thin films of composition $Cr_{70}Fe_{30}$ and $Cr_{75}Fe_{25}$ have been chosen for this purpose.

2. Experimental details

$Cr_{75-x}Fe_{25+x}$ ($x = 0, 5$) thin films were grown on 100 μm thick glass substrate by 1 keV Ar ion-beam sputtering from a $2'' \times 2''$ well-homogenized targets of composition $Cr_{75}Fe_{25}$ and $Cr_{70}Fe_{30}$. Cu-K_α x-ray reflectivity, measured using BRUKER x-ray diffractometer, confirmed the high quality of the films. A typical x-ray reflectivity (XRR) data for the $Cr_{70}Fe_{30}$ films with thickness t = 42 nm and 21 nm are displayed in Fig. 1. LEPTOS simulation of the observed XRR patterns, yielded the thickness values of the $Cr_{70}Fe_{30}$ films as t = 978(2), 417(3), 157(3), 88(2), 42(2), 21(2) and 11(2) nm. The $Cr_{75}Fe_{25}$ thin films also have similar thicknesses.

2.1. Structural analysis

Room temperature x-ray diffraction (XRD) pattern taken in the grazing incident angle mode on the $Cr_{70}Fe_{30}$ film with $t = 417$ nm is depicted in Fig. 2. The inset highlights the weaker intensity Bragg peaks. The measured XRD pattern, when fitted with the profile matching (Full Proof), yields the lattice parameter value $a = 0.28737(1)$ nm for $Cr_{70}Fe_{30}$. This value compares favorably with that ($a = 0.2889(3)$ nm) reported [20] for the $Cr_{69}Fe_{31}$ thin film with thickness $t \simeq 220$ nm. The most intense peak in Fig. 2 corresponds to the (110) Bragg reflection. The average grain size (D) calculated using the Scherrer formula [21] for the above-mentioned thin film, is 20(1) nm. Fig. 3 displays the atomic force micrographs of the $Cr_{70}Fe_{30}$ films with thickness $t = 417$ nm, 88 nm, 21 nm and 11 nm. A columnar grain growth along the film normal is observed in all the films, more so in the film with the lowest thickness. In the atomic force micrograph of the film with t = 417 nm, many grains have the size 20(1) nm.

The details of synthesis and characterization are furnished elsewhere [15–19]. Real and imaginary components of the linear (χ_1) and nonlinear ($\chi_2 - \chi_5$) ac-magnetic susceptibilities have been

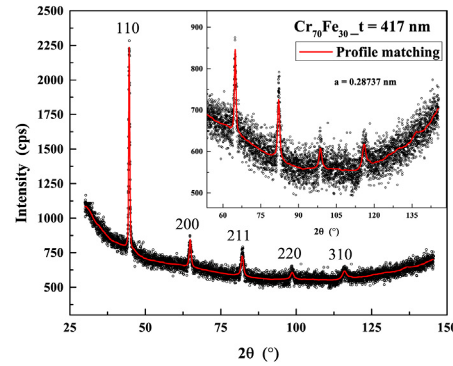

Fig. 2. Grazing incident-angle x-ray diffraction pattern of the $Cr_{70}Fe_{30}$ thin film of thickness $t = 417$ nm. Inset shows the enlarged view of the weak intensity Bragg peaks occurring at higher angles.

measured on the $Cr_{70}Fe_{30}$ disc-shaped (5 mm in diameter) thin films at the ac driving-fields of rms amplitude $h_{ac} = 1$ Oe, 5 Oe and 10 Oe over three decades of frequency ($10^1 - 10^4$ Hz) in the temperature range $2\ K \le T \le 300$ K. Irrespective of the ac-driving field frequency, ω, the imaginary components for all the thin film samples are an order of magnitude smaller than their real counterparts only in the case of linear ac-susceptibility, χ_1. The real component thus essentially equals the total χ_1. However, the relative magnitudes of the real and imaginary components of nonlinear ac-susceptibility depend on ω; higher the order of susceptibility, more sensitive the relative magnitudes are to ω. Note that $\chi_1(T) = \chi_1{}'(T)$ = (temperature-dependent magnetic moment in emu)/h_{ac} while $\chi_n(T) = \chi_n{}'(T)\ h_{ac}^{n-1}$, where $\chi_1{}'$ and $\chi_n{}'$ with $n = 2, 3, 4, 5$ are the real components of the linear and nonlinear susceptibilities. The structural characterization and measurement of the ac magnetic response, $\chi_1(T,\omega) - \chi_5(T,\omega)$, on the $Cr_{75}Fe_{25}$ thin films are in progress. In this paper, only the results obtained on the $Cr_{70}Fe_{30}$ thin films are presented.

3. Results and discussion

3.1. Scaling equation of state analysis

All the panels in Figs. 4 and 5, and more so their insets, highlight the effect of the static biasing field, H_{dc}, on the temperature variation of the linear ac susceptibility, $\chi_1(T)$, in $Cr_{70}Fe_{30}$ thin films of thickness $t \ge 88$ nm (Fig. 4) and $t \le 42$ nm (Fig. 5). For example, in the film with thickness t = 978 nm (as in other thicknesses) the 'zero-field' (H_{dc} = 0) susceptibility shows a Hopkinson peak at around $T \approx 160$ K, that progressively broadens and shifts to lower

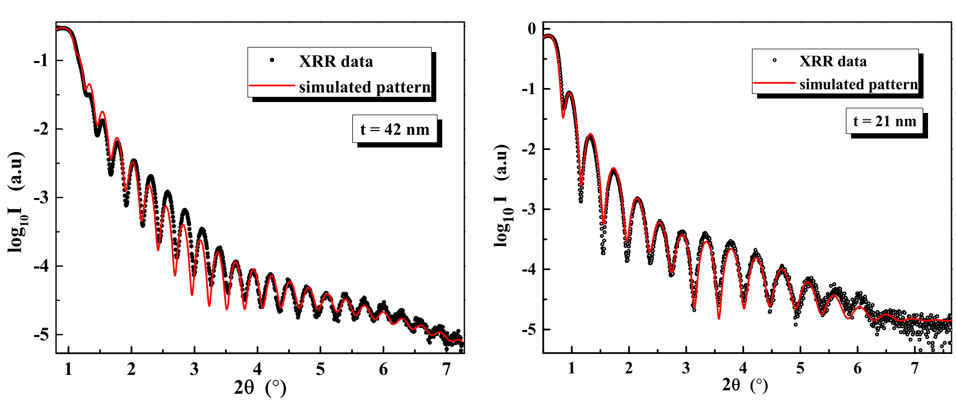

Fig. 1. The x-ray reflectivity data along with LEPTOS simulated fits for the $Cr_{70}Fe_{30}$ films with thickness t = 42 nm and 21 nm.